Discovery of non-classical complex models between a cationic water-soluble pillar[6]arene and naphthalenesulfonate derivatives and their self-assembling behaviors

Mengbin Wang and Jiong Zhou*

Department of Chemistry, Zhejiang University, Hangzhou 310027, P. R. China; Fax and Tel: +86-571-8795-3189;
Email address: jiongzhou@zju.edu.cn

Electronic Supplementary Information (30 pages)

1. Materials and methods

All reagents were commercially available and used as supplied without further purification. Solvents were either employed as purchased or dried according to procedures described in the literature. Compound **H**[S1] was synthesized according to published literature procedures. NMR spectra were recorded with a Bruker Avance DMX 400 spectrophotometer or a Bruker Avance DMX 500 spectrophotometer with the deuterated solvent as the lock and the residual solvent or TMS as the internal reference. Isothermal titration calorimetry (ITC) experiments were performed on a VP-ITC micro-calorimeter (Microcal, USA). Transmission electron microscopy (TEM) investigations were carried out on a JEM-1200EX instrument. The fluorescence experiments were conducted on a RF-5301 spectrofluorophotometer (Shimadzu Corporation, Japan). UV-vis absorption spectra were recorded by a PerkinElmer Lambda 35 UV-vis spectrophotometer. Dynamic light scattering (DLS) was carried out on a Malvern Nanosizer S instrument at room temperature.

2. Partial ^1H NMR spectra for 1:1 complex study

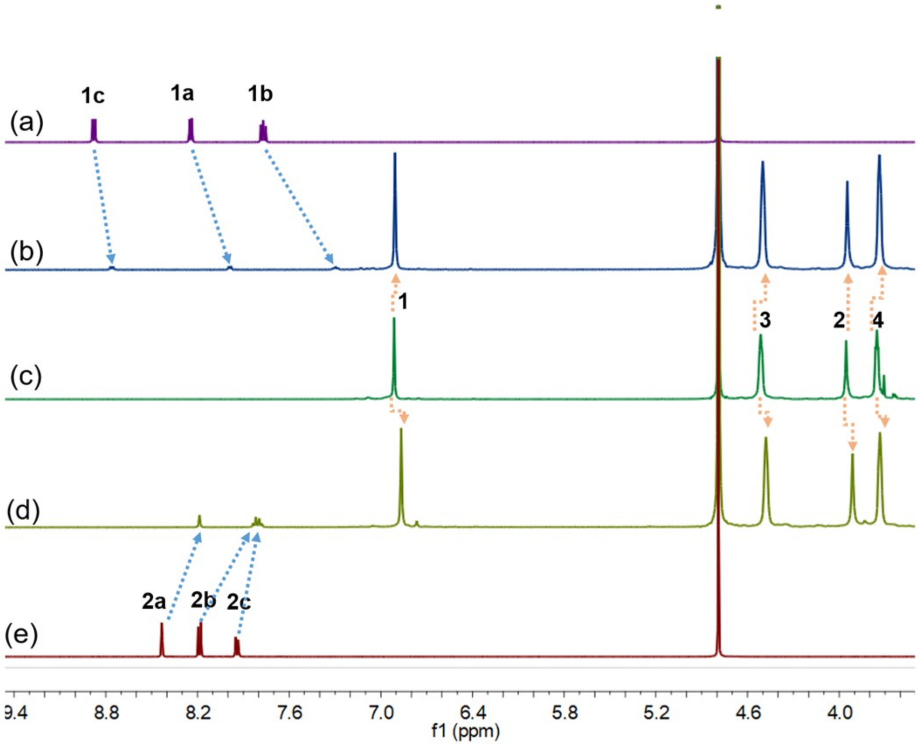

Fig. S1 Partial ^1H NMR spectra (500 MHz, D_2O, 293 K) of (a) **G1** (5.00 mM); (b) **G1** (1.00 mM) + **H** (5.00 mM); (c) **H** (1.00 mM); (d) **G2** (1.00 mM) + **H** (5.00 mM); (e) **G2** (5.00 mM).

*3. Partial 2D COSY spectra of **G3** and **G4***

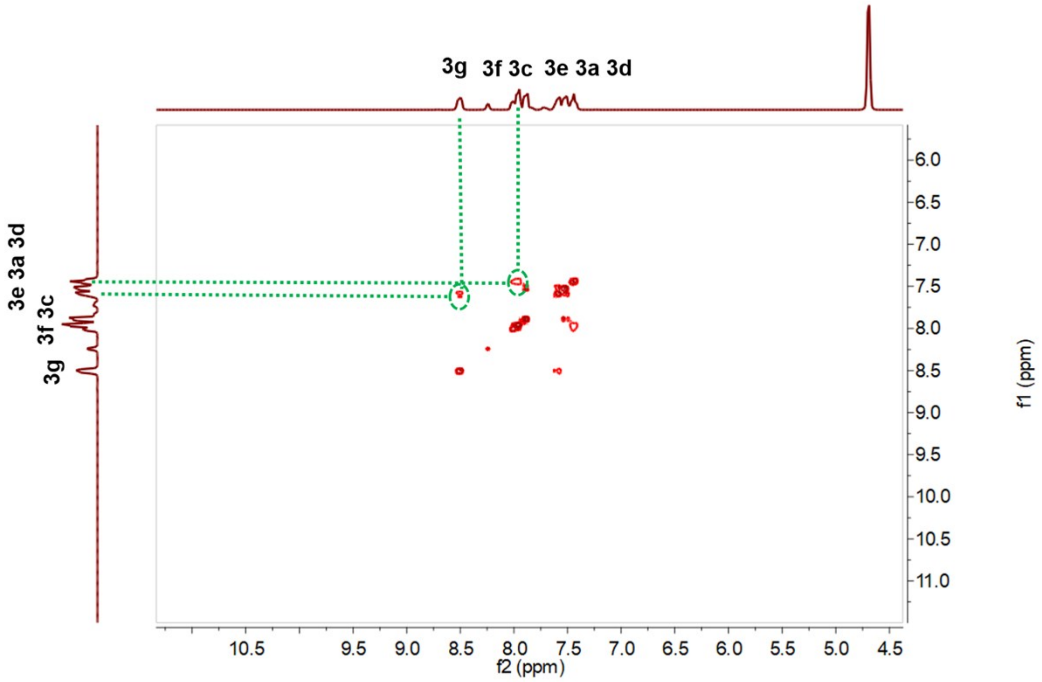

Fig. S2 Partial 2D COSY NMR spectrum (400 MHz, D_2O, 293 K) of **G4** (25.0 mM).

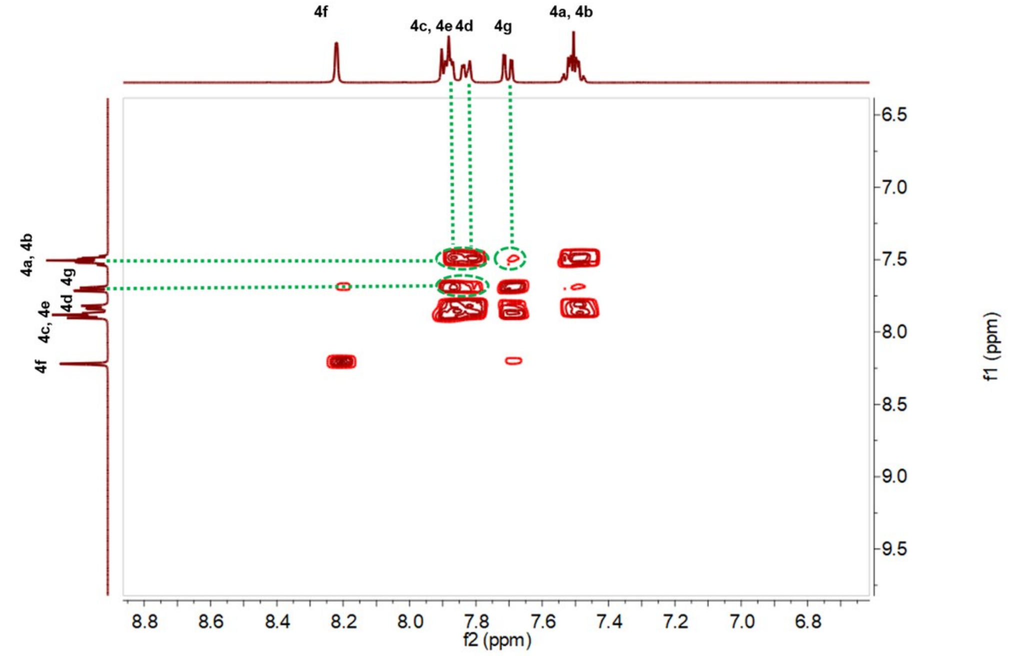

Fig. S3 Partial 2D COSY NMR spectrum (400 MHz, D_2O, 293 K) of **G4** (25.0 mM).

4. Fluorescence spectroscopy study

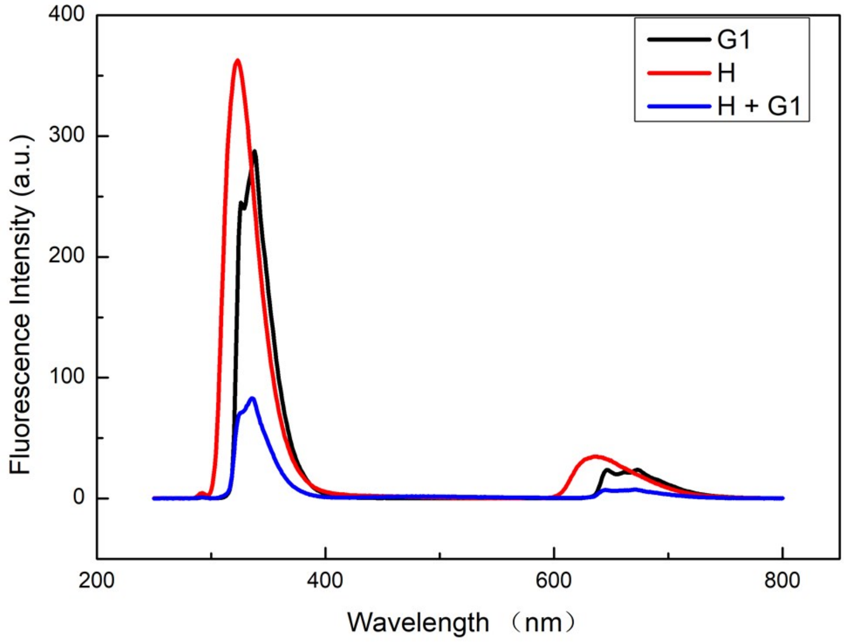

Fig. S4 Fluorescence spectra (λ_{ex} = 290 nm) of **H** (0.0500 mM), **G1** (0.0500 mM) and **H** (0.0500 mM) + **G1** (0.100 mM).

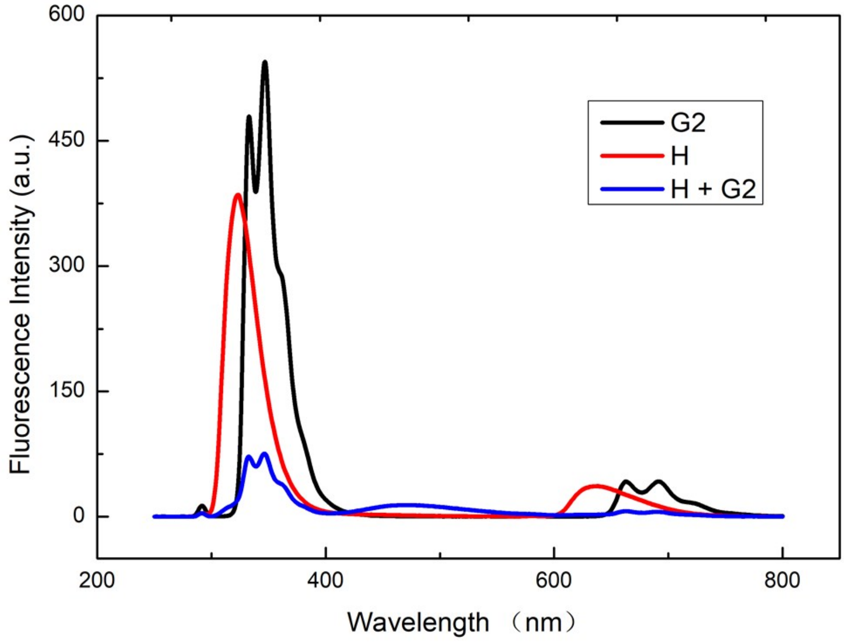

Fig. S5 Fluorescence spectra (λ_{ex} = 290 nm) of **H** (0.0500 mM), **G2** (0.0500 mM) and **H** (0.0500 mM) + **G2** (0.100 mM).

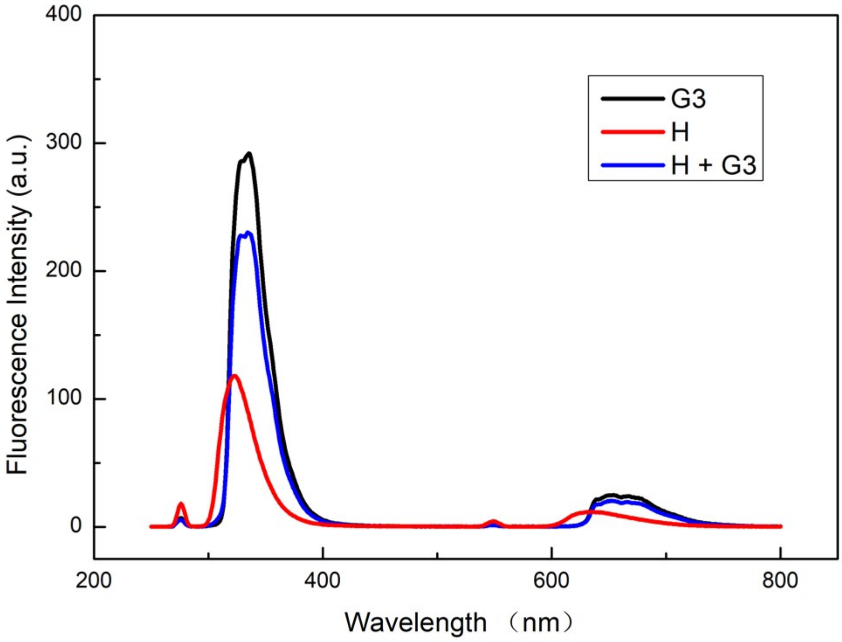

Fig. S6 Fluorescence spectra (λ_{ex} = 272 nm) of **H** (0.0500 mM), **G3** (0.0500 mM) and **H** (0.0500 mM) + **G3** (0.0500 mM).

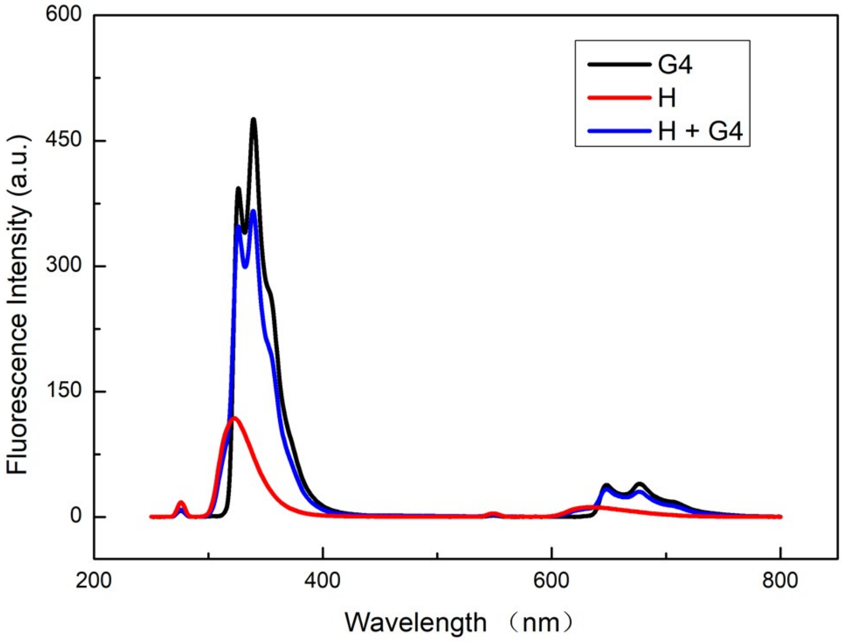

Fig. S7 Fluorescence spectra (λ_{ex} = 272 nm) of **H** (0.0500 mM), **G4** (0.0500 mM) and **H** (0.0500 mM) + **G4** (0.0500 mM).

5. UV-vis absorption spectropy study

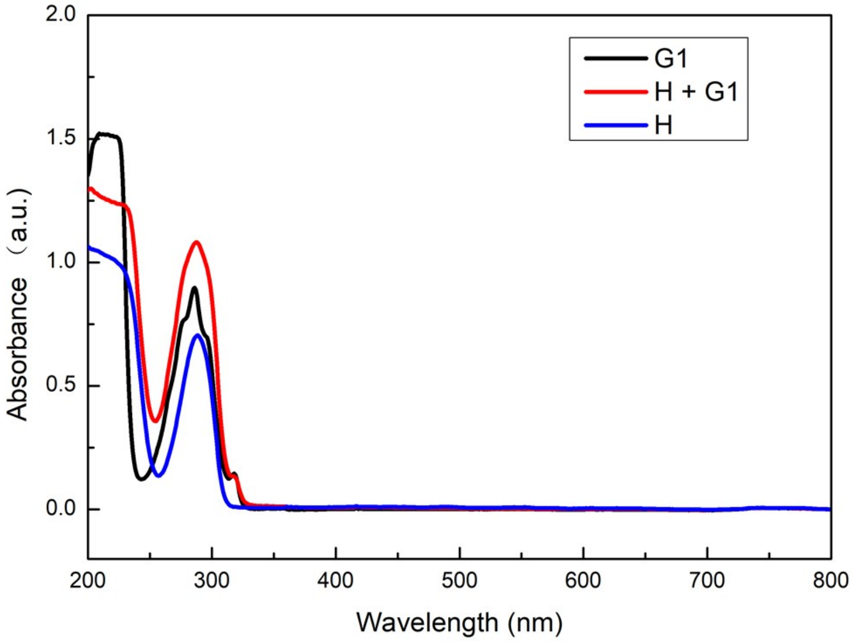

Fig. S8 UV-vis absorption spectra of **H** (0.0500 mM), **G1** (0.0500 mM) and **H** (0.0500 mM) + **G1** (0.100 mM).

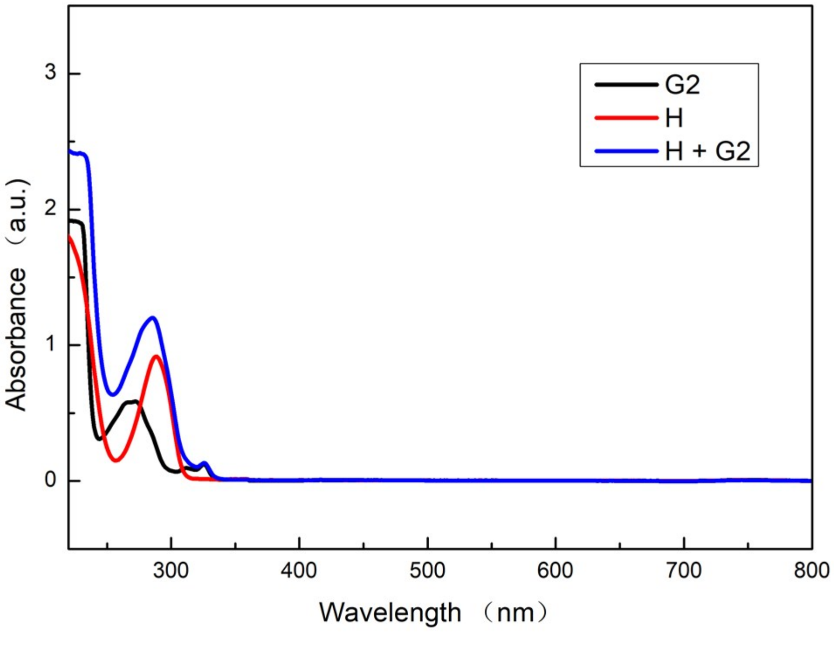

Fig. S9 UV-vis absorption spectra of **H** (0.0500 mM), **G2** (0.0500 mM) and **H** (0.0500 mM) + **G2** (0.100 mM).

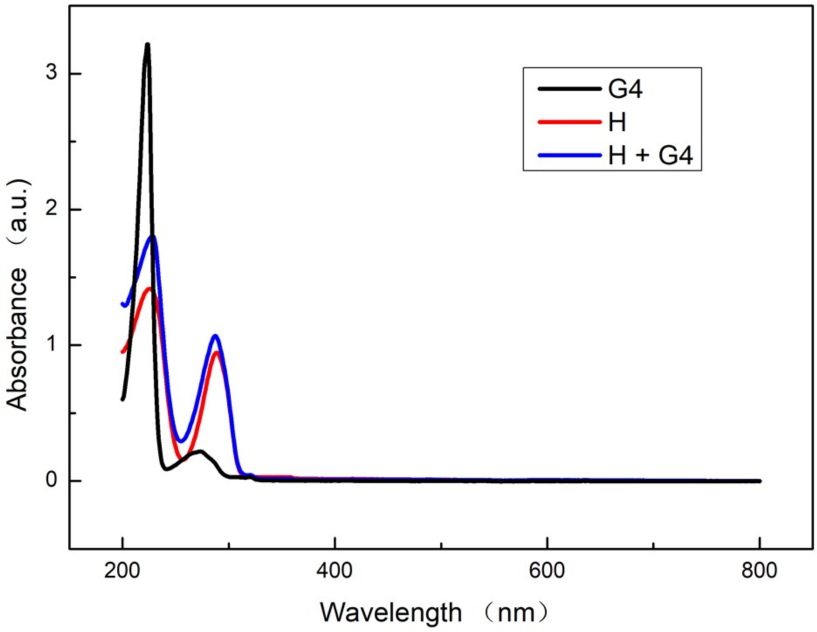

Fig. S10 UV-vis absorption spectra of **H** (0.0500 mM), **G3** (0.0500 mM) and **H** (0.0500 mM) + **G3** (0.0500 mM).

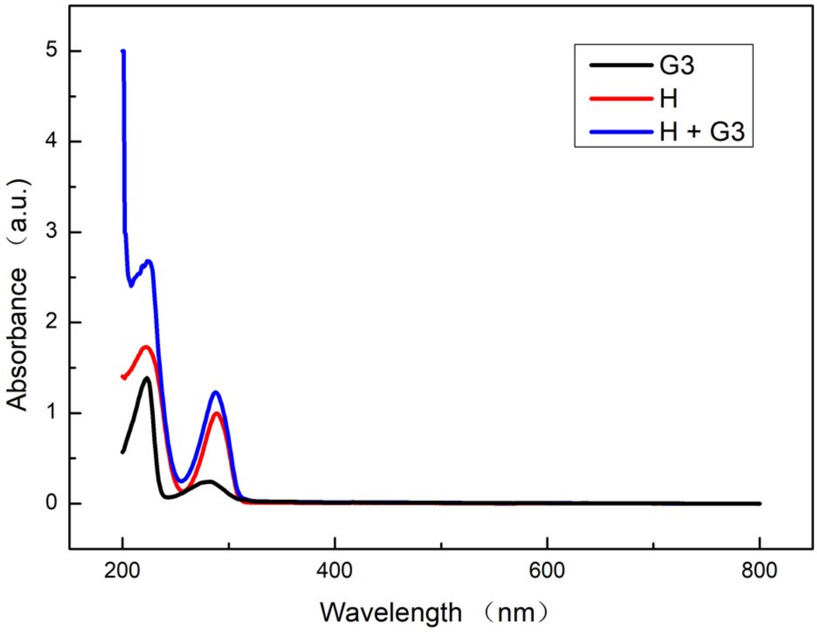

Fig. S11 UV-vis absorption spectra of **H** (0.0500 mM), **G4** (0.0500 mM) and **H** (0.0500 mM) + **G4** (0.0500 mM).

*6. 2D NOESY spectra of **H⊃G1**, **H⊃G3** and **H⊃G4***

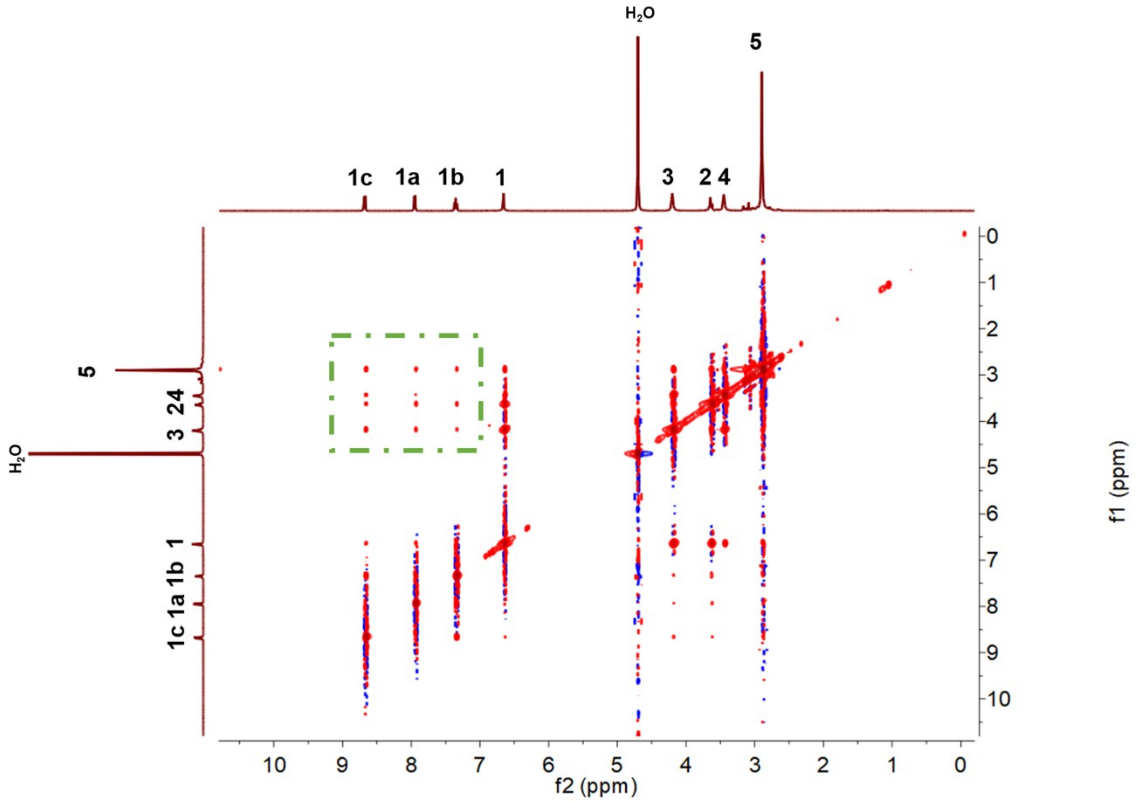

Fig. S12 2D NOESY NMR spectrum (500 MHz, D_2O, 293 K) of **H** (5.00 mM) with **G1** (25.0 mM).

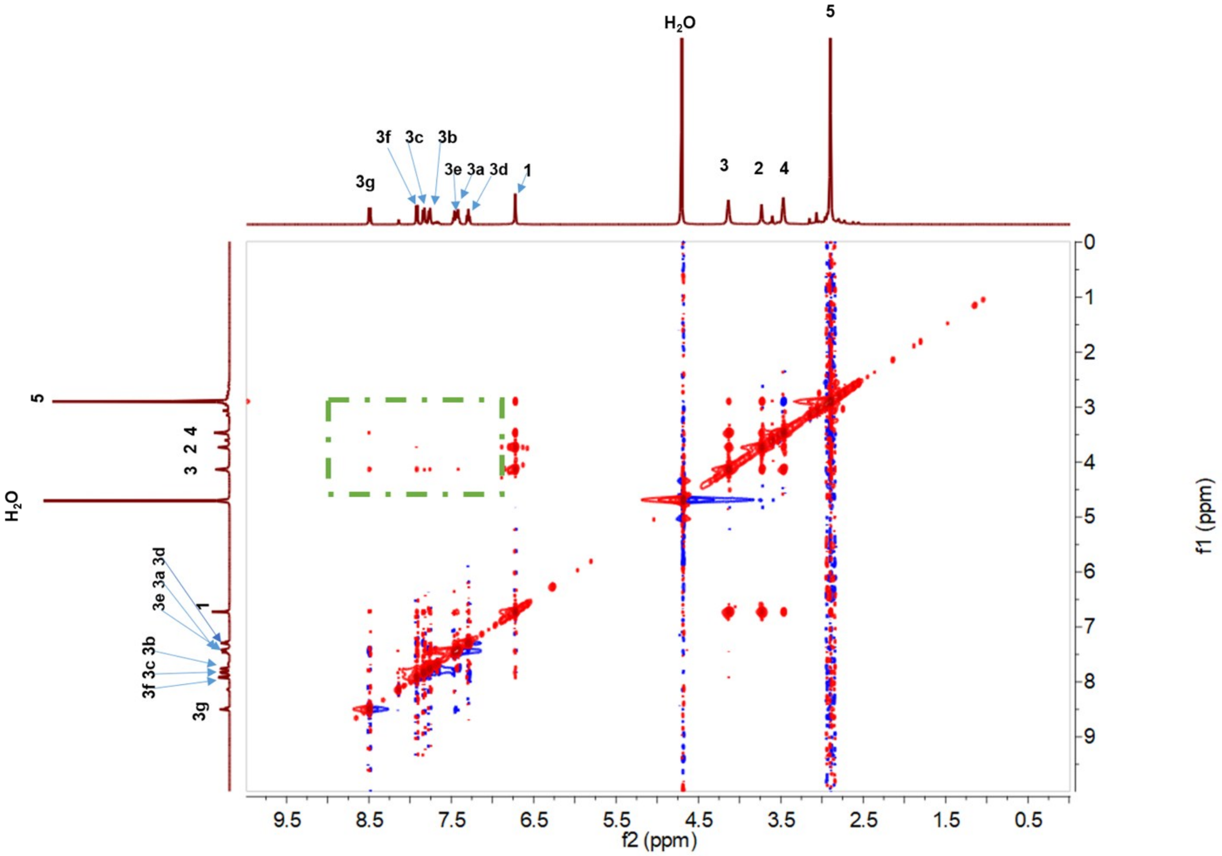

Fig. S13 2D NOESY NMR spectrum (500 MHz, D_2O, 293 K) of **H** (5.00 mM) with **G3** (25.0 mM).

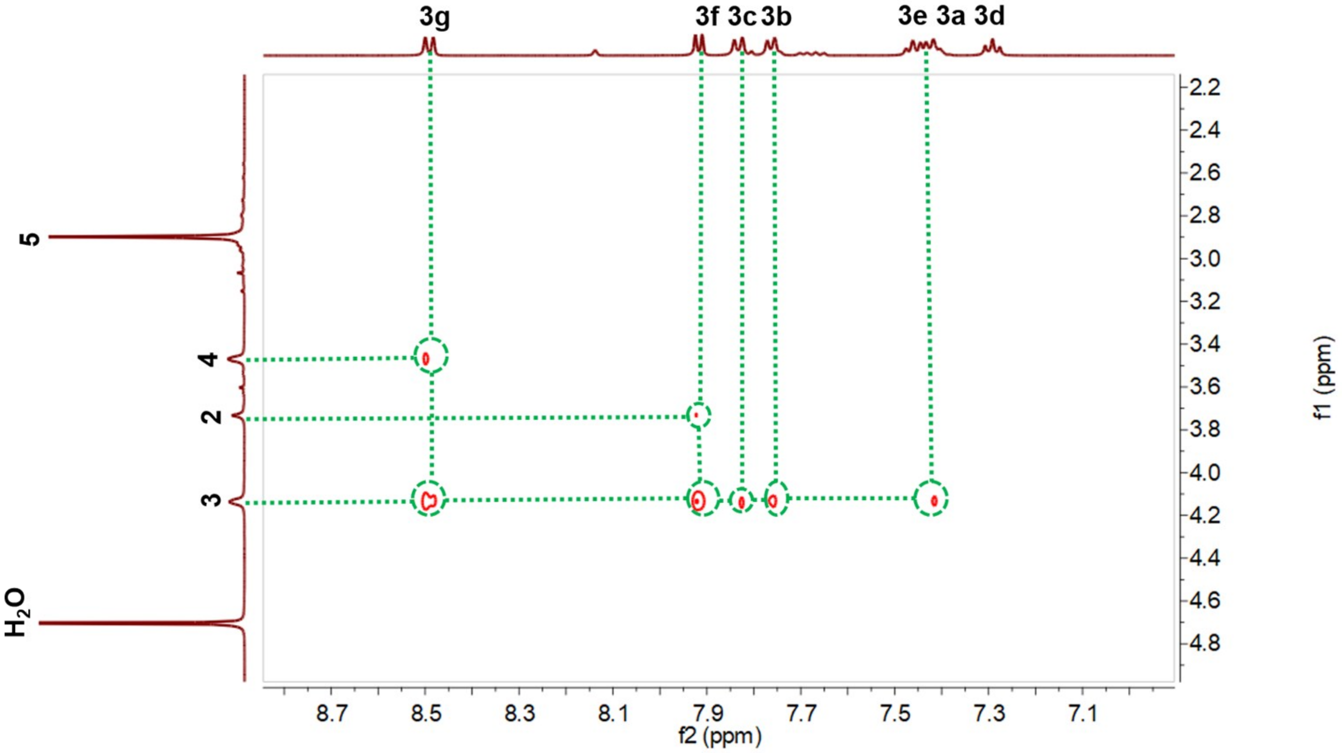

Fig. S14 Partial 2D NOESY NMR spectrum (500 MHz, D_2O, 293 K) of **H** (5.00 mM) with **G3** (25.0 mM).

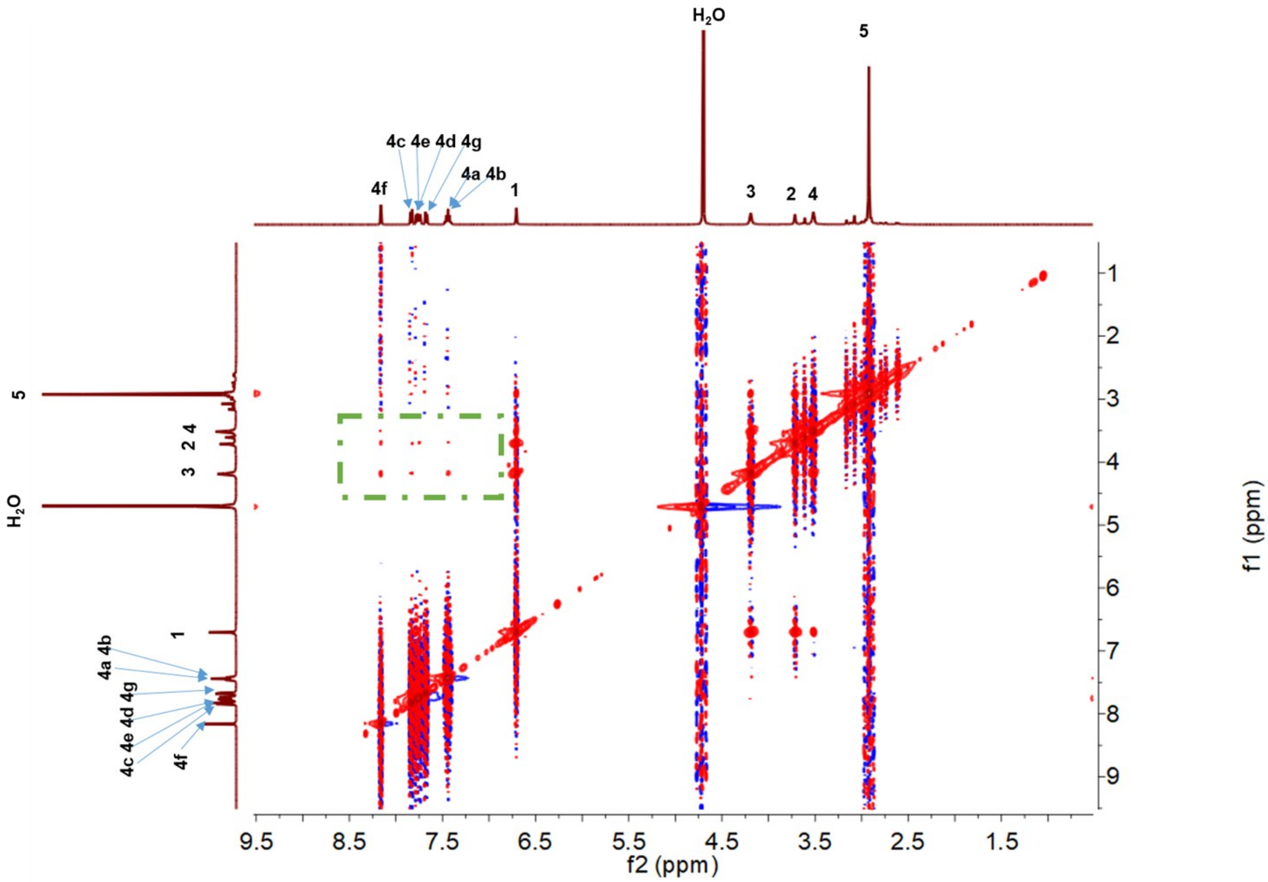

Fig. S15 2D NOESY NMR spectrum (500 MHz, D_2O, 293 K) of **H** (5.00 mM) with **G4** (25.0 mM).

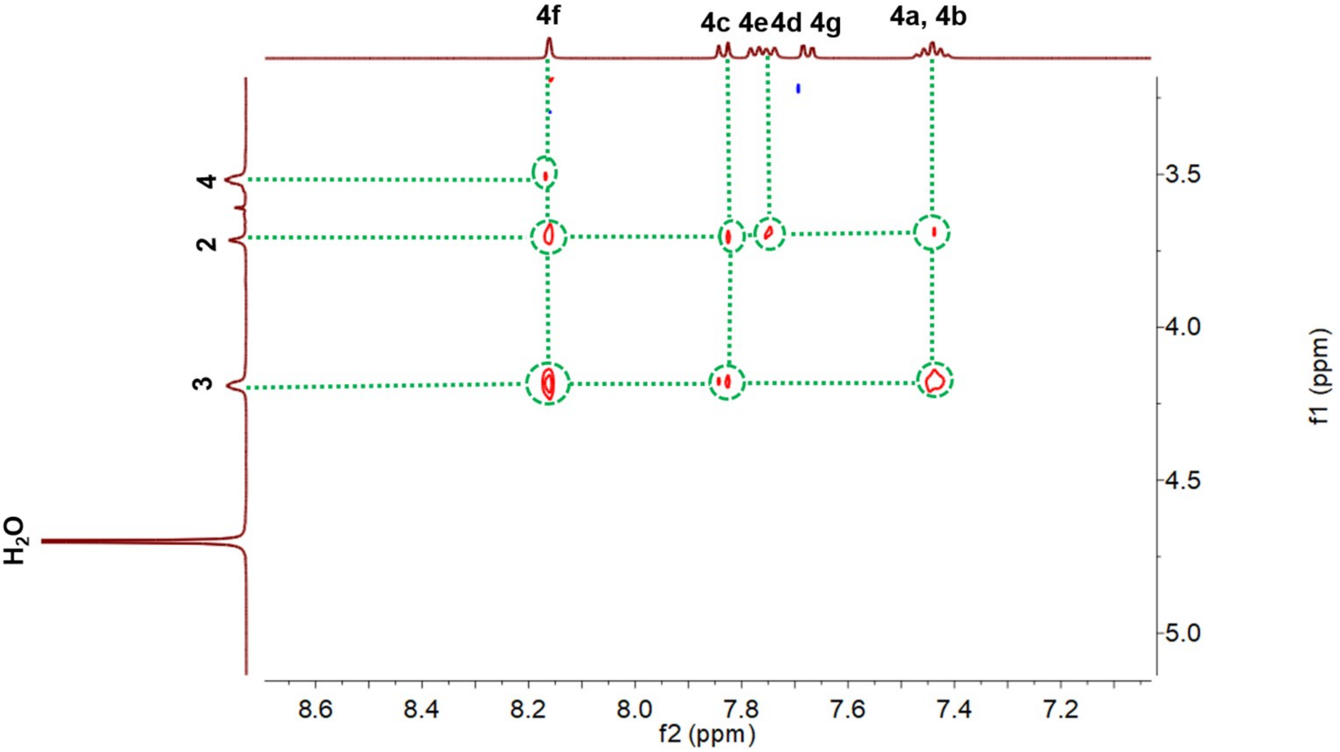

Fig. S16 Partial 2D NOESY NMR spectrum (500 MHz, D_2O, 293 K) of **H** (5.00 mM) with **G4** (25.0 mM).

*7. ITC results of **H⊃G3** and **H⊃G4***

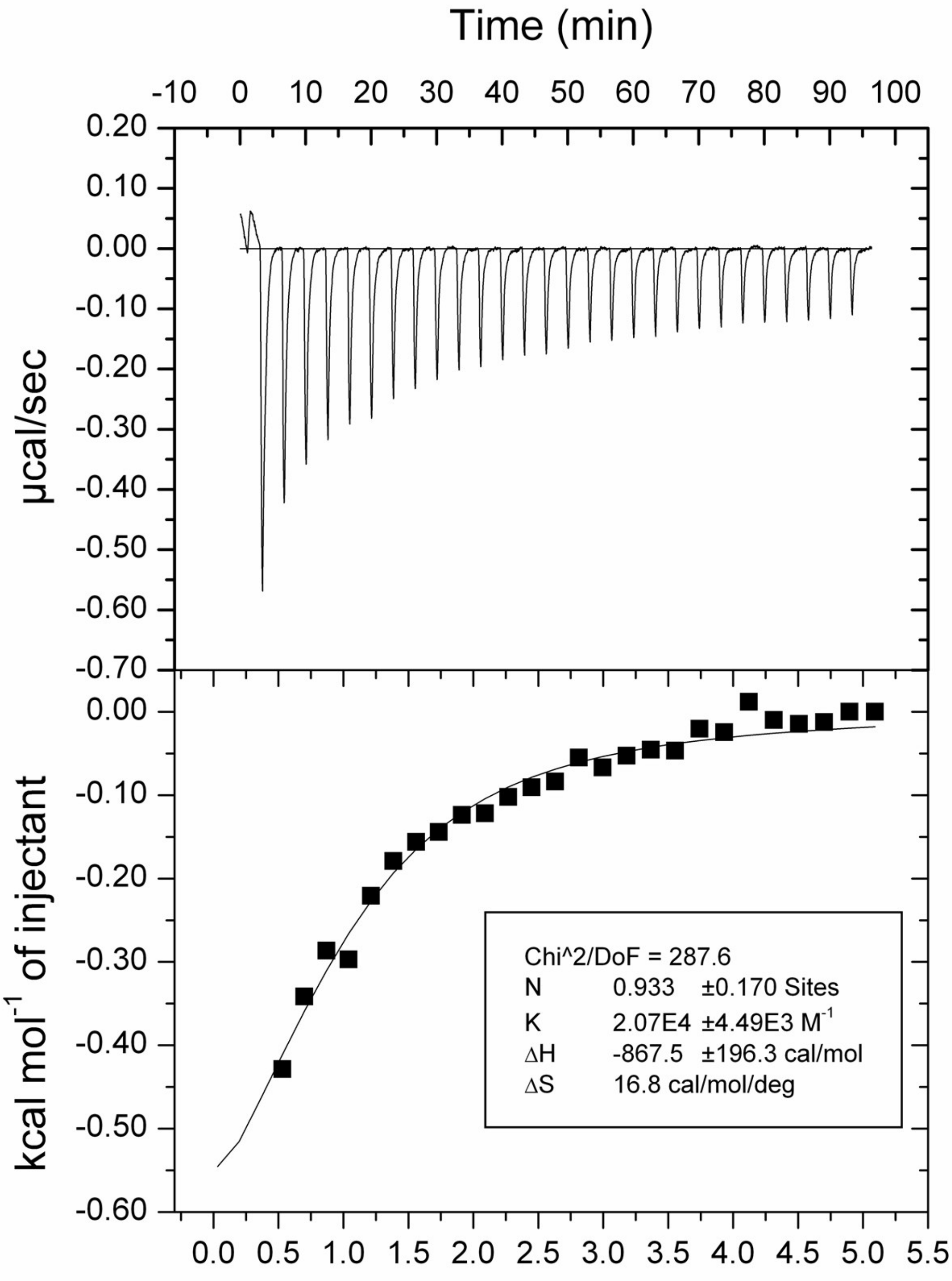

Fig. S17 Microcalorimetric titration experiment of **H** with **G3** at 298 K. (Top) Raw ITC data for 29 sequential injections (10 μL per injection) of **G3** solution (2.00 mM) into **H** (0.100 mM) solution. (Bottom) Net reaction heat obtained from the integration of the calorimetric traces.

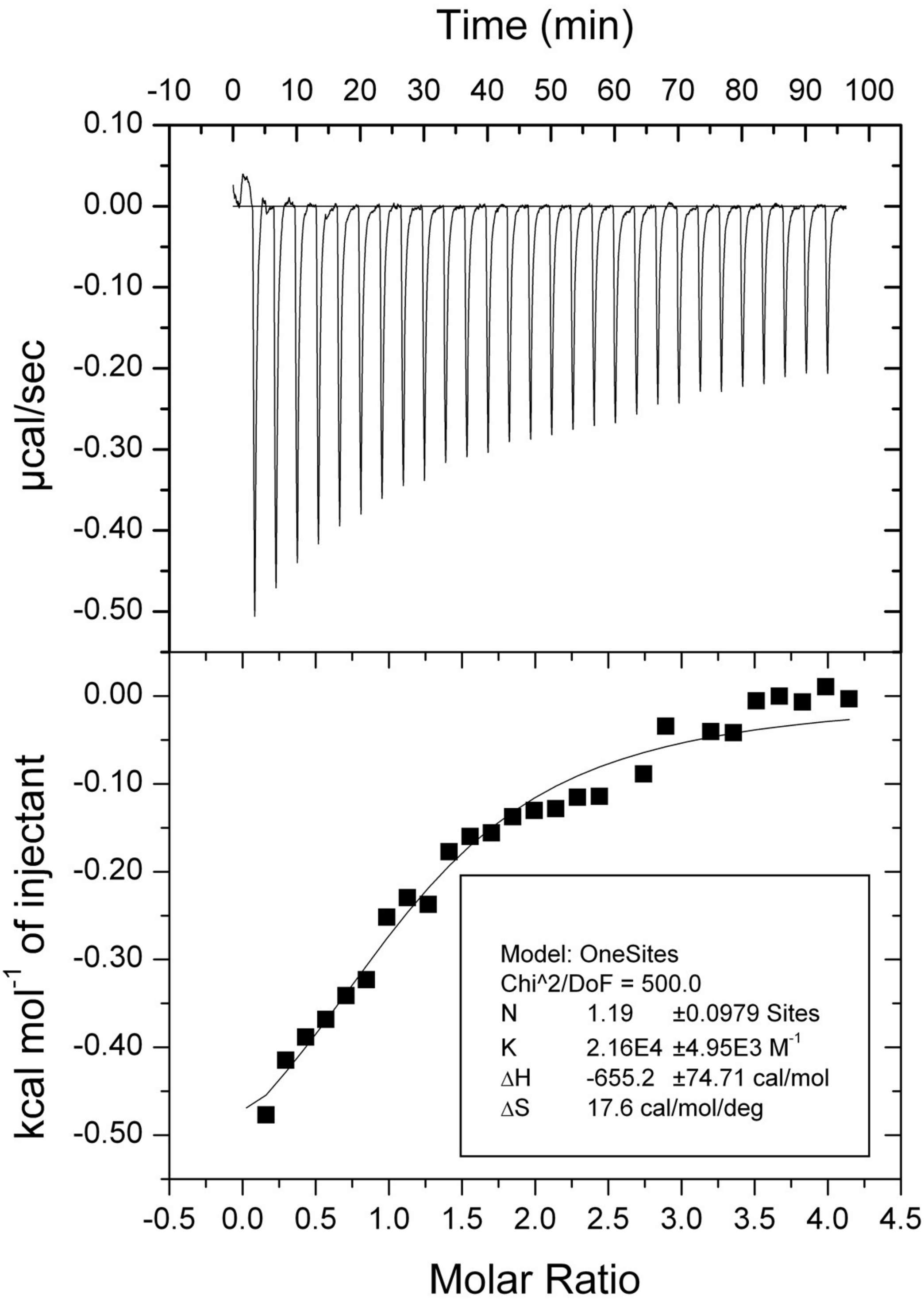

Fig. S18 Microcalorimetric titration experiment of **H** with **G4** at 298 K. (Top) Raw ITC data for 29 sequential injections (10 µL per injection) of **G4** solution (2.00 mM) into **H** (0.100 mM) solution. (Bottom) Net reaction heat obtained from the integration of the calorimetric traces.

8. ^{1}H NMR titration experiments

^{1}H NMR titration experiments were carried out with the concentration of **H** kept constant at 1.00 mM and that of guests varied at 293 K. The molar ratio plot showed that the complex ratio of **H⊃G1** and **H⊃G2** was 1:2. The association constants (K_a) of them were estimated by a non-linear curve-fitting method with the equation: [S2]

$$\Delta\delta = (\Delta\delta_{\mathrm{HG}} K_1 [\mathrm{G}] + \Delta\delta_{\mathrm{HG2}} K_1 K_2 [\mathrm{G}]^2)/(1 + K_1 [\mathrm{G}] + K_1 K_2 [\mathrm{G}]^2) \qquad \text{Eq. 1}$$

Where $\Delta\delta$ is the chemical shift change of H_3 on **H** at different concentration of guest, $\Delta\delta_{\mathrm{HG}}$ is the chemical shift change of H_3 when **H** is completely complexed by the first guest molecule, $\Delta\delta_{\mathrm{HG2}}$ is the chemical shift change of H_3 when **H** is completely complexed by the second guest molecule, and [G] is the concentration of guest molecule.

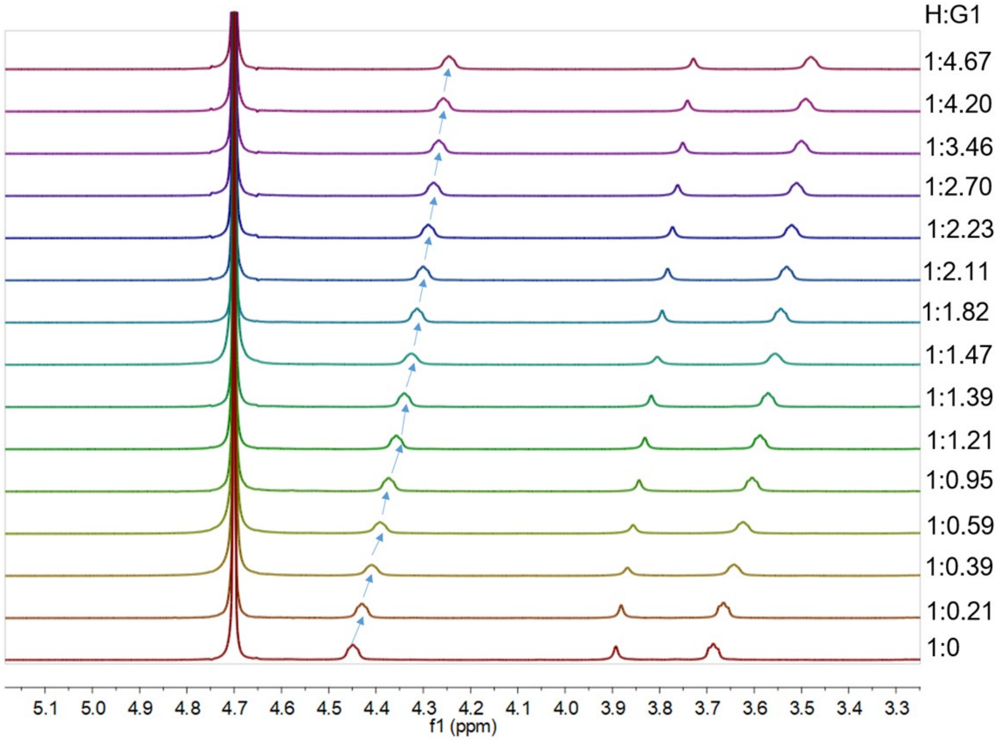

Fig. S19 Partial ^{1}H NMR spectra of **H** (1.00 mM) in the presence of increasing amounts of **G1** in D_2O at 293 K.

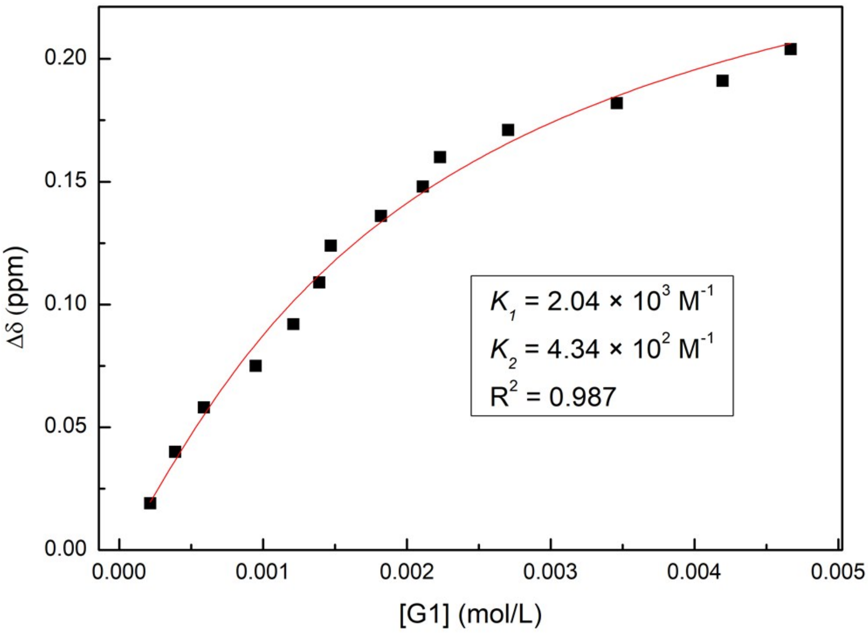

Fig. S20 Molar ratio plot for the binding of **H** with **G1** in D_2O at 293 K.

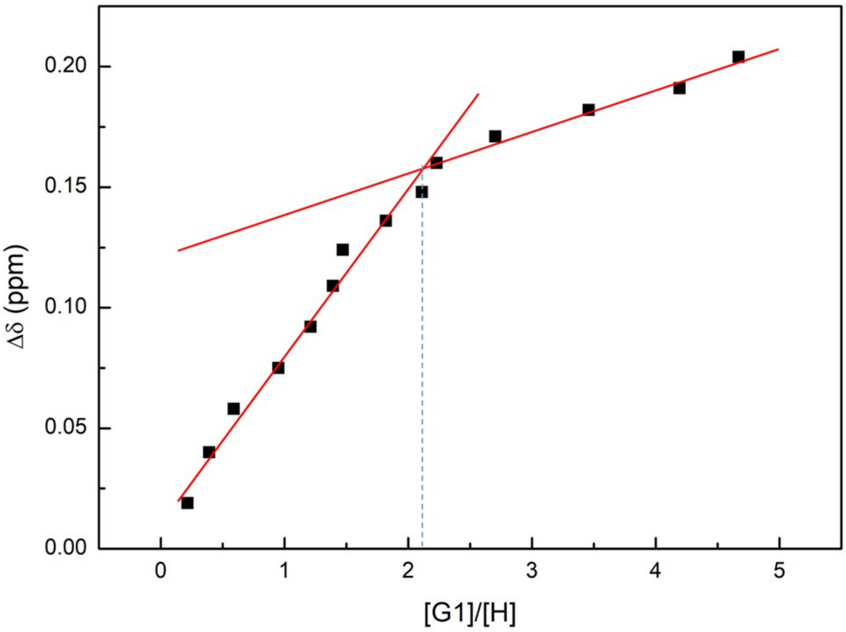

Fig. S21 Changes of the chemical shift changes of H_3 on **H** with addition of **G1**. The red solid line was obtained from the non-linear curve-fitting with Eq. 1.

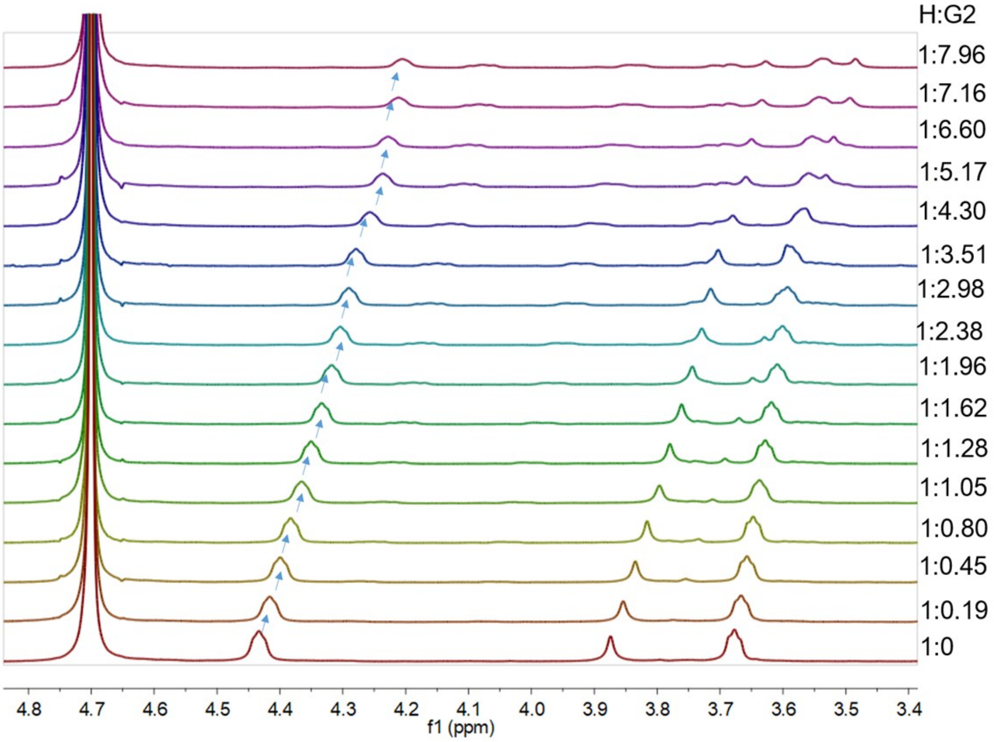

Fig. S22 Partial ^{1}H NMR spectra of **H** (1.00 mM) in the presence of increasing amounts of **G2** in D_2O at 293 K.

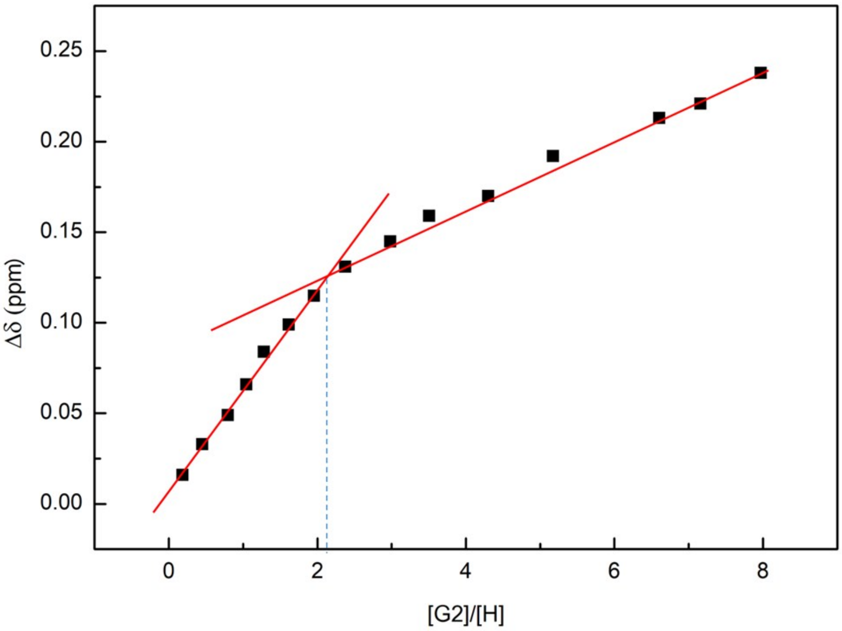

Fig. S23 Molar ratio plot for the binding of **H** with **G2** in D_2O at 293 K.

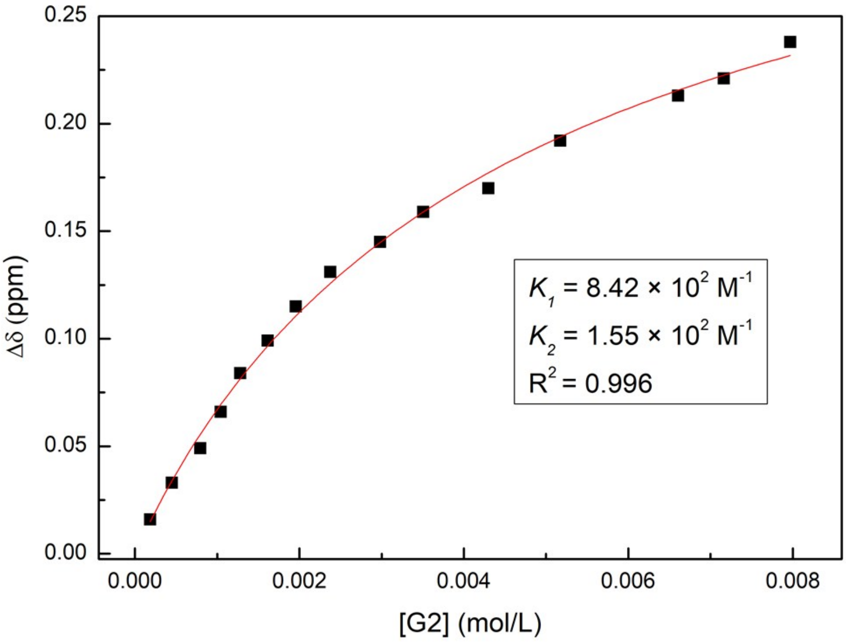

Fig. S24 Changes of the chemical shift changes of H_3 on **H** with addition of **G2**. The red solid line was obtained from the non-linear curve-fitting with Eq. 1.

According to the molar ratio plot, a 1:1 stoichiometry was obtained for **H** binding with **G3** and **G4**. The association constants (K_a) were estimated by a non-linear curve-fitting method with the equation: [S2]

$$\Delta\delta = (\Delta\delta_\infty/[H]_0)(0.5[G] + 0.5([H]_0+1/K_a) - (0.5([G]^2 + (2[G]\,(1/K_a - [H]_0)) + (1/K_a + [H]_0)^2)^{0.5})) \qquad \text{Eq. 2}$$

Where $\Delta\delta$ is the chemical shift change of H_3 on **H** at different concentration of guest, $\Delta\delta_\infty$ is the chemical shift change of H_3 when **H** is completely complexed, $[H]_0$ is the fixed initial concentration of the host, and [G] is the concentration of guest molecule.

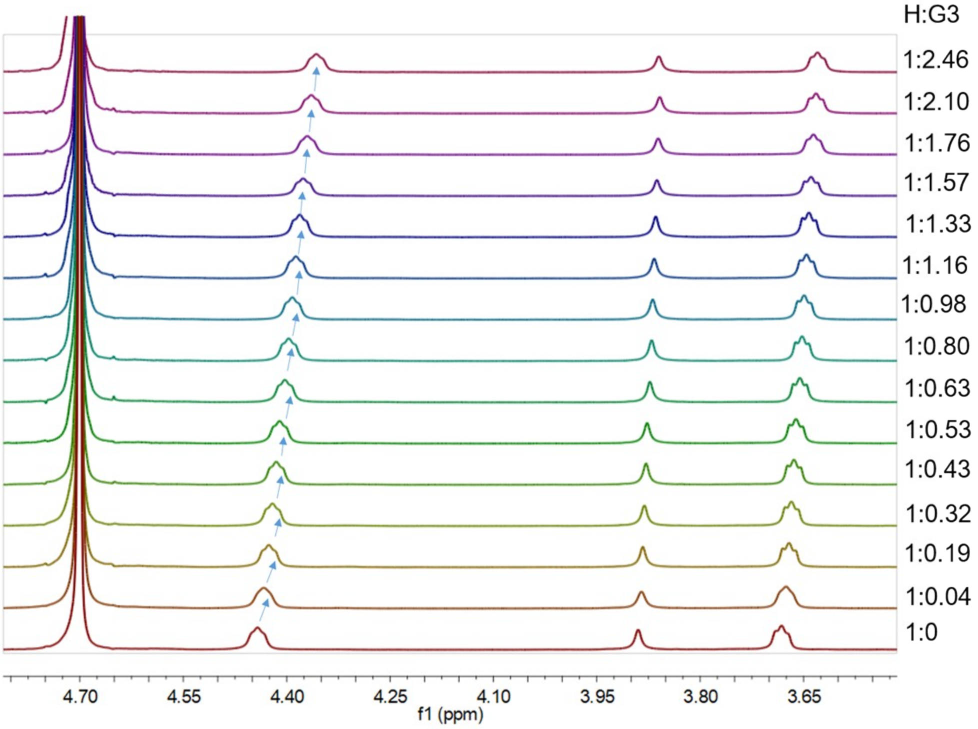

Fig. S25 Partial ^{1}H NMR spectra of **H** (1.00 mM) in the presence of increasing amounts of **G3** in D_2O at 293 K.

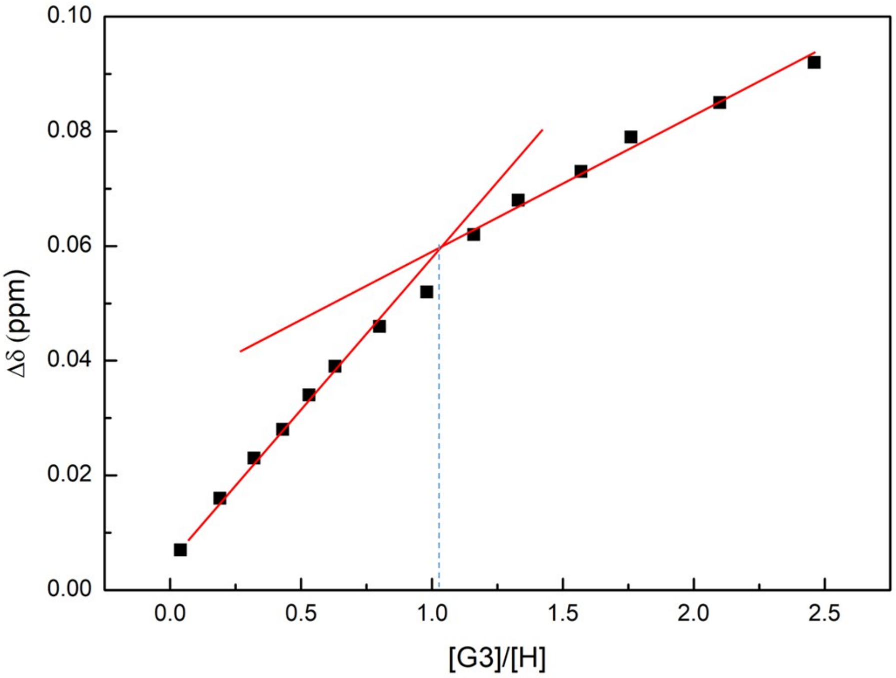

Fig. S26 Molar ratio plot for the binding of **H** with **G3** in D_2O at 293 K.

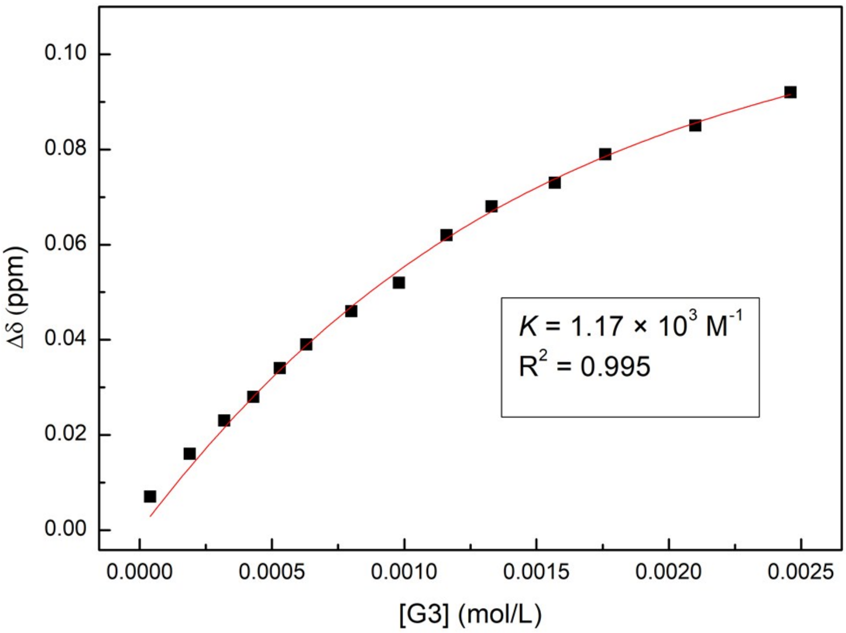

Fig. S27 Changes of the chemical shift of H_3 on **H** with addition of **G3**. The red solid line was obtained from the non-linear curve-fitting with Eq. 2.

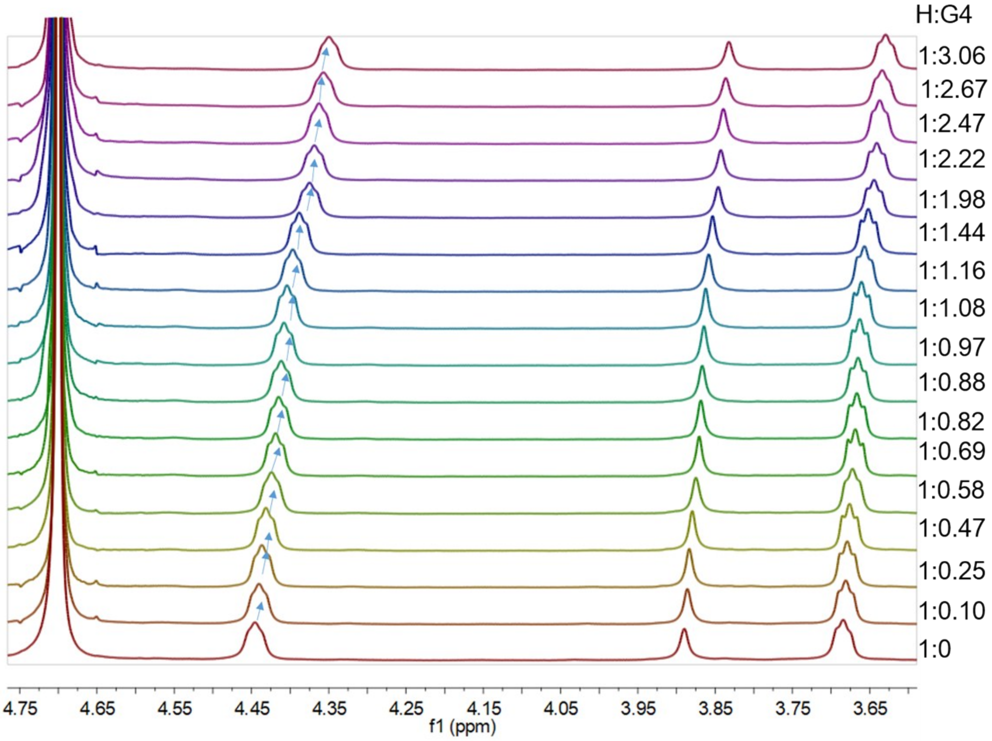

Fig. S28 ^{1}H NMR spectra of **H** (1.00 mM) in the presence of increasing amounts of **G4** in D_2O at 293 K.

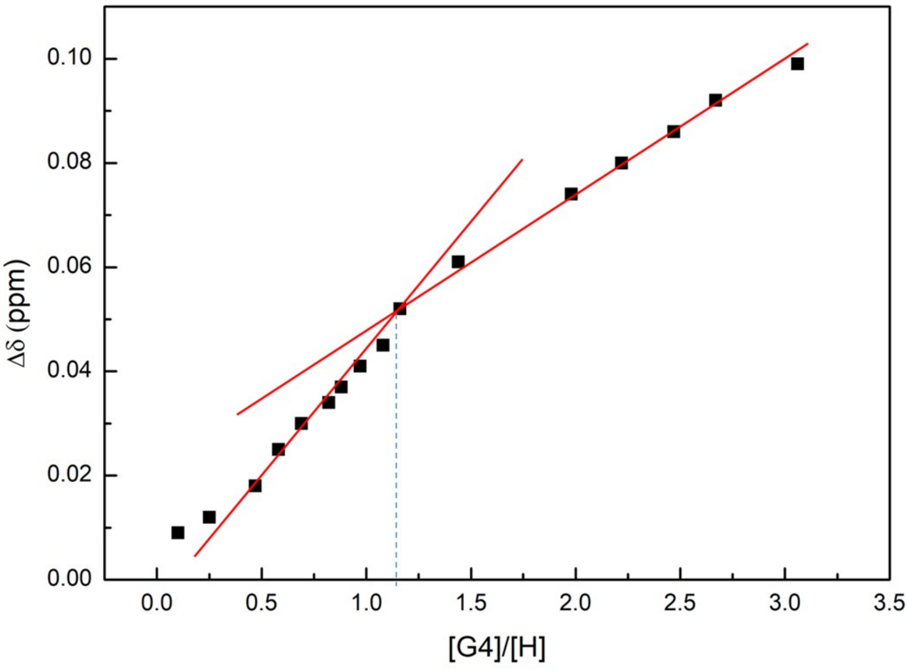

Fig. S29 Molar ratio plot for the binding of **H** with **G4** in D_2O at 293 K.

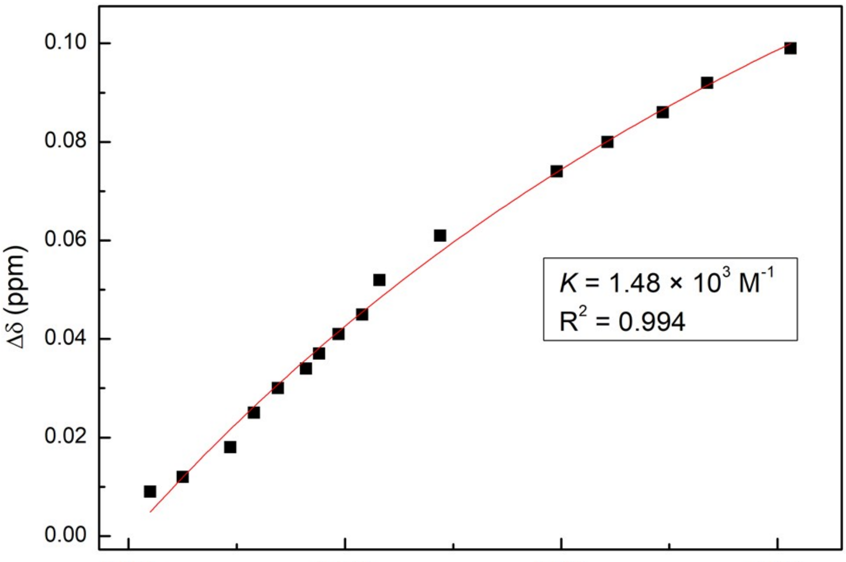

Fig. S30 Changes of the chemical shift of H_3 on **H** with addition of **G4**. The red solid line was obtained from the non-linear curve-fitting with Eq. 2.

9. Fluorescence titration experiments

Fluorescence titration experiments were done. For **G1** and **G2**, fluorescence titration experiments were carried out in water solutions which had a constant concentration of **H** (0.0500 mM) and varying concentration of guests (**G1**, **G2**), and the association constants of them were estimated by a non-linear curve-fitting method with the Eq. 3.[S2]

$$\Delta F = (\Delta F_{\mathrm{HG}} K_1 [\mathrm{G}] + \Delta F_{\mathrm{HG2}} K_1 K_2 [\mathrm{G}]^2)/(1 + K_1 [\mathrm{G}] + K_1 K_2 [\mathrm{G}]^2) \qquad \text{Eq. 3}$$

Where ΔF is the emission intensity change of **H** at 330 nm, ΔF_{HG} is the emission intensity change when **H** is completely complexed by the first guest molecule, ΔF_{HG2} is the emission intensity change when **H** is completely complexed by the second guest molecule, and [G] is the concentration of guest molecule.

For **G3**, fluorescence titration experiment was performed by increasing the concentration of **H** with a constant concentration of **G3** (0.0500 mM), and the association constant (Ka) was estimated by a non-linear curve-fitting method with the Eq. 4.[S2]

$$\Delta F = (\Delta F_{\infty}/[\mathrm{G}]_0)(0.5[\mathrm{G}] + 0.5([\mathrm{G}]_0+1/K_a) - (0.5([\mathrm{H}]^2 + (2[\mathrm{H}]\,(1/K_a - [\mathrm{G}]_0)) + (1/K_a + [\mathrm{G}]_0)^2)^{0.5})) \qquad \text{Eq. 4}$$

Where ΔF is the emission intensity change of **G3** at 305 nm at different concentration of **H**, ΔF_{∞} is the emission intensity change when **H** is completely complexed, $[\mathrm{G}]_0$ is the fixed initial concentration of **G3**, and [H] is the concentration of **H**.

For **G4**, fluorescence titration experiments were performed by increasing the concentration of **H** with a constant concentration of **G4** (0.0500 mM), and the association constant (Ka) was estimated by the Stern-Volmer equation:[S3]

$$\ln (F_0/ F - 1) = \ln Ka + n\ln [\mathrm{G}] \qquad \text{Eq. 5}$$

where F_0 is the initial fluorescent emission intensity of guest at 341 nm and F is the fluorescent emission intensity of guest in the presence of different concentrations of **H**.

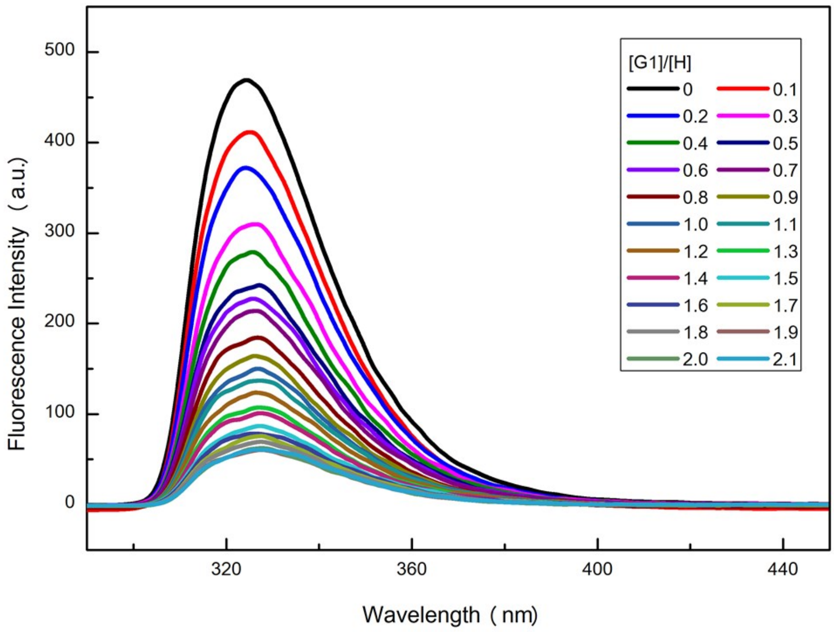

Fig. S31 Fluorescence spectra of **H** at a concentration of 5.00 × 10^{-5} M in aqueous solution at room temperature with different concentrations of **G1**.

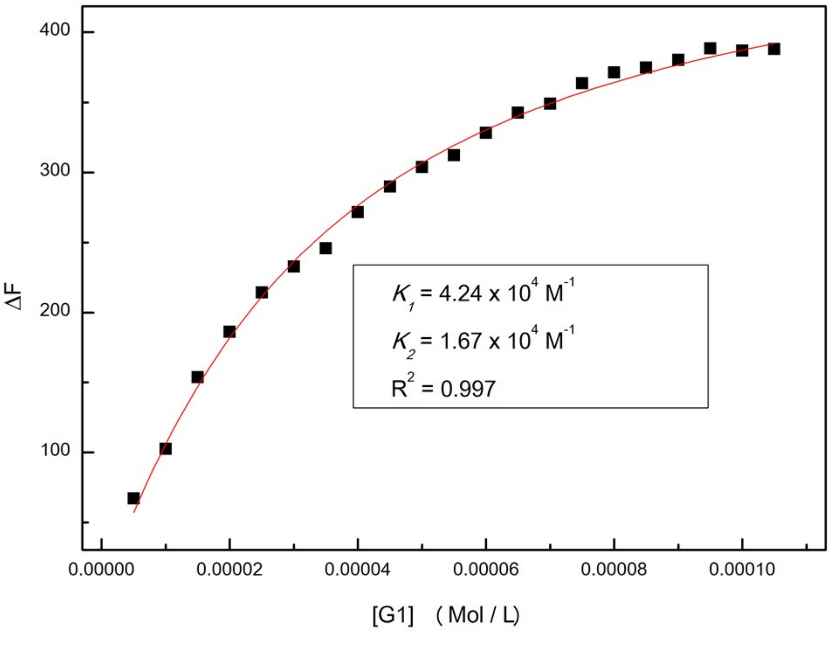

Fig. S32 The fluorescence intensity changes of **H** with different concentrations of **G1**. The red solid line was obtained from the non-linear curve-fitting with Eq. 3.

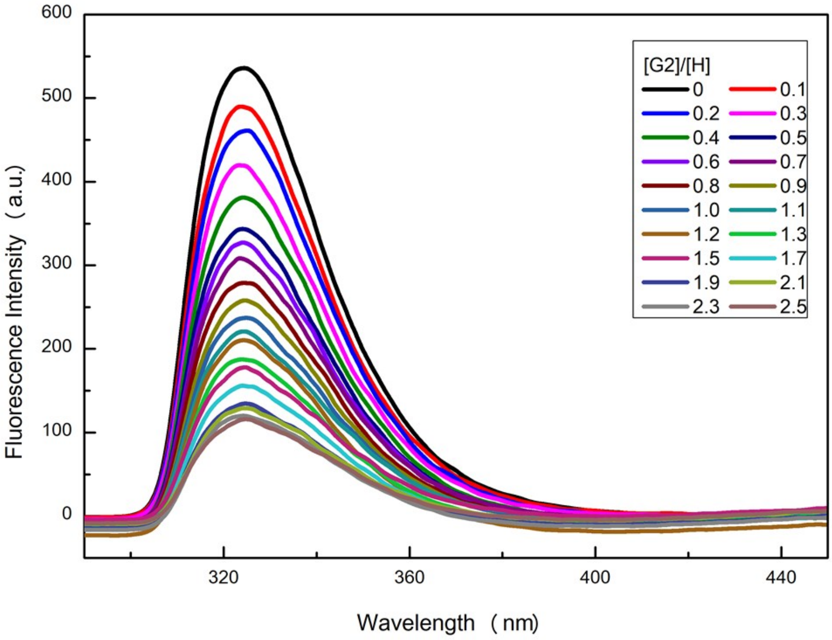

Fig. S33 Fluorescence spectra of **H** at a concentration of 5.00×10^{-5} M in aqueous solution at room temperature with different concentrations of **G2**.

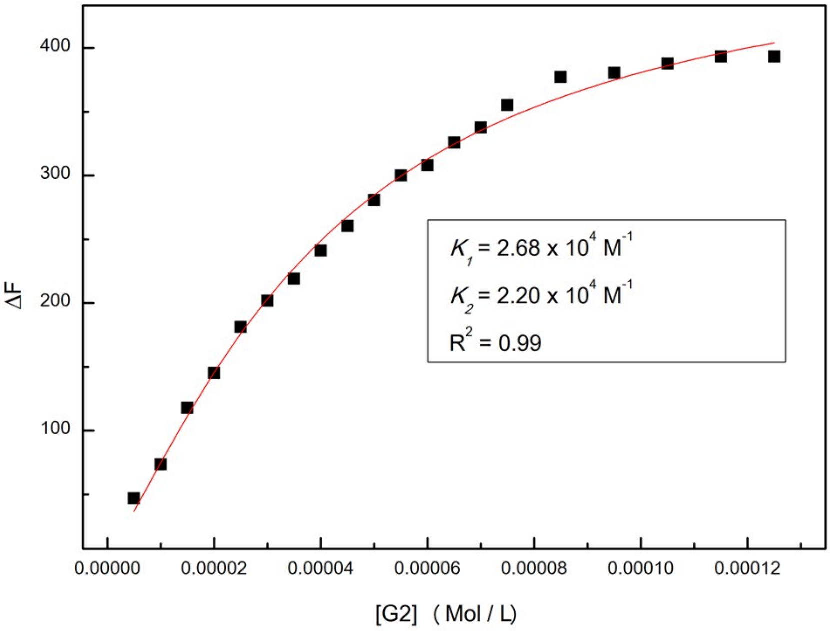

Fig. S34 The fluorescence intensity changes of **H** with different concentrations of **G2**. The red solid line was obtained from the non-linear curve-fitting with Eq. 3.

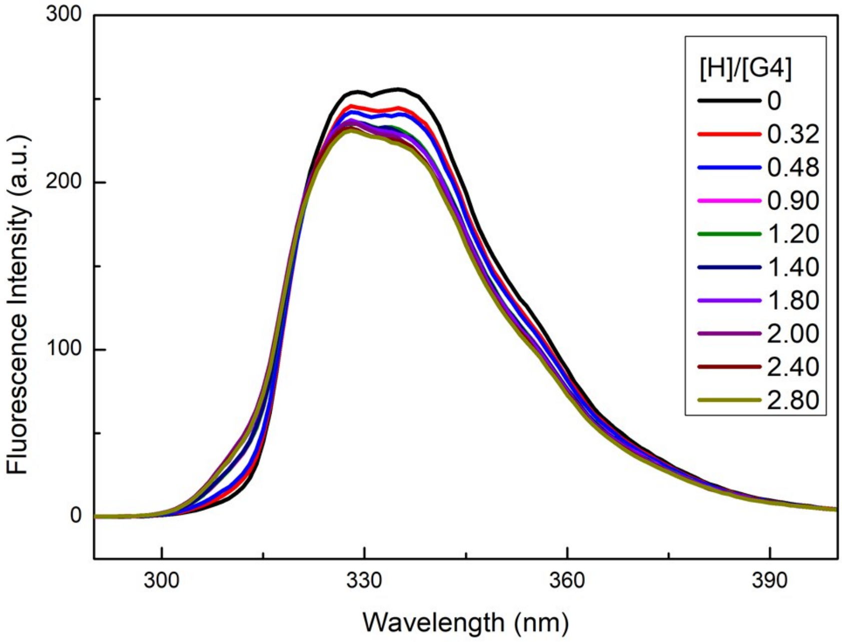

Fig. S35 Fluorescence spectra of **G3** at a concentration of 5.00 × 10^{-5} M in aqueous solution at room temperature with different concentrations of **H**.

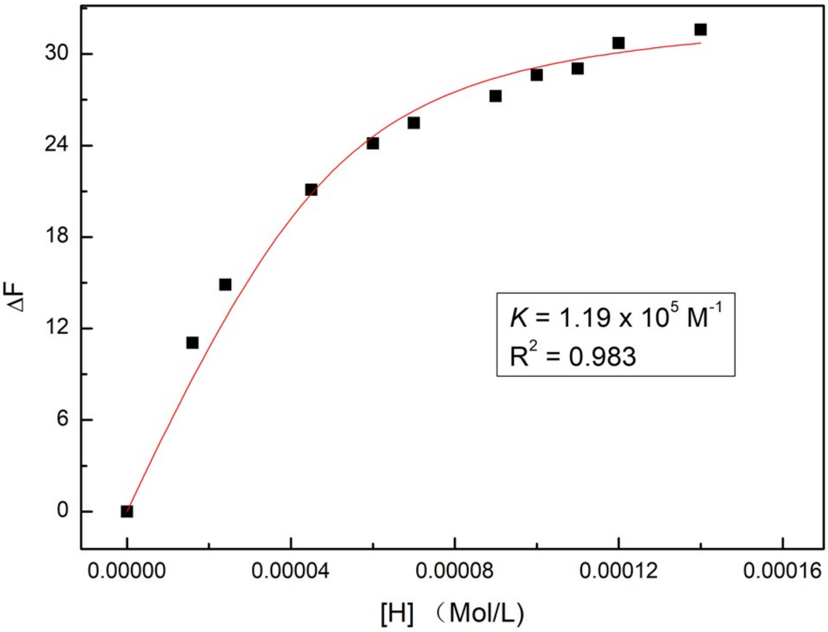

Fig. S36 The fluorescence intensity changes of **G3** with different concentrations of **H**. The red solid line was obtained from the non-linear curve-fitting with Eq. 4.

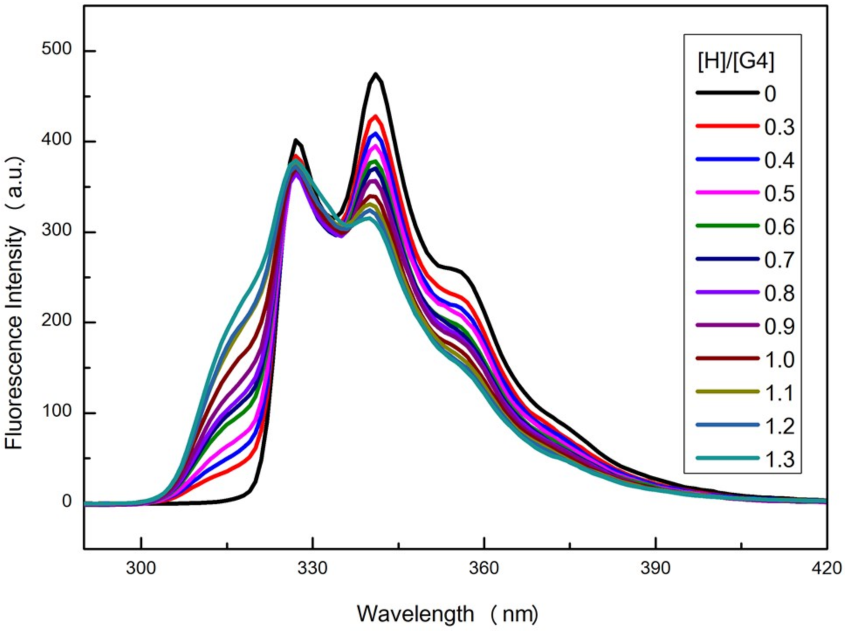

Fig. S37 Fluorescence spectra of **G4** at a concentration of 5.00×10^{-5} M in aqueous solution at room temperature with different concentrations of **H**.

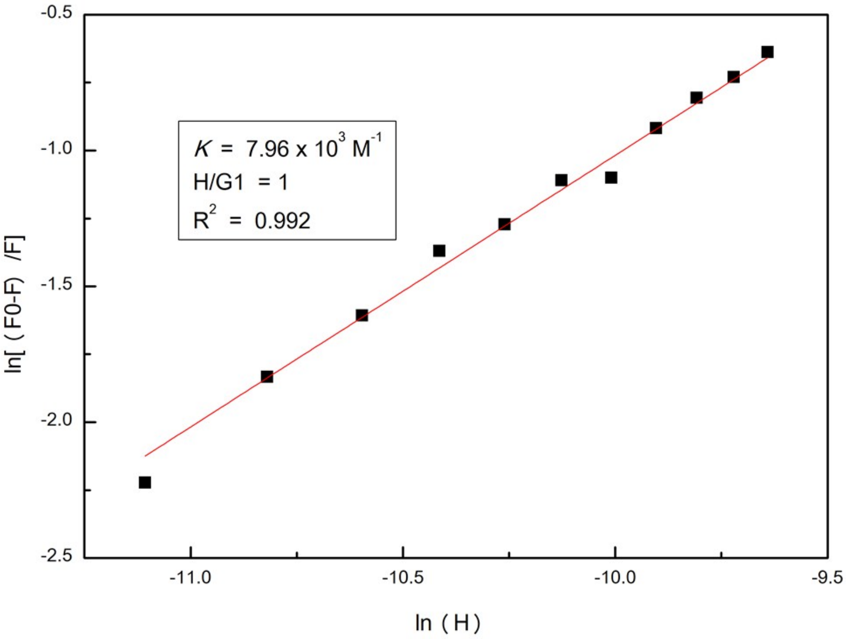

Fig. S38 The plot of the Stern-Volmer equation for the binding of **H** with **G4**. The red solid line was obtained from the non-linear curve-fitting with Eq. 5.

*9. TEM images of single **H** and **G2***

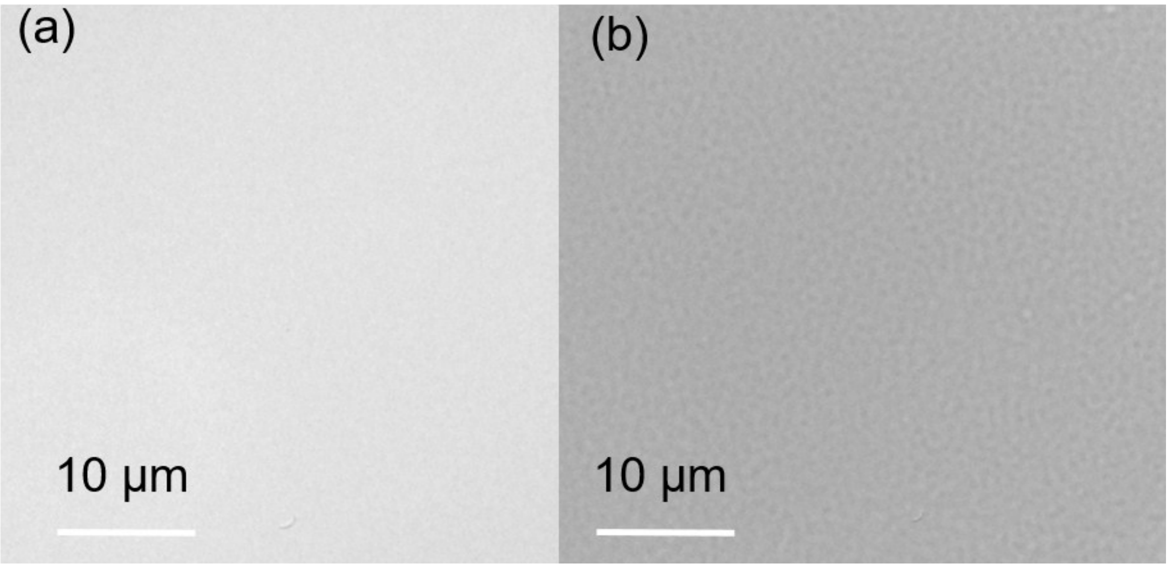

Fig. S39 TEM images of single **H** (a) and **G2** (b).

*10. DLS study of **H⊃G2***

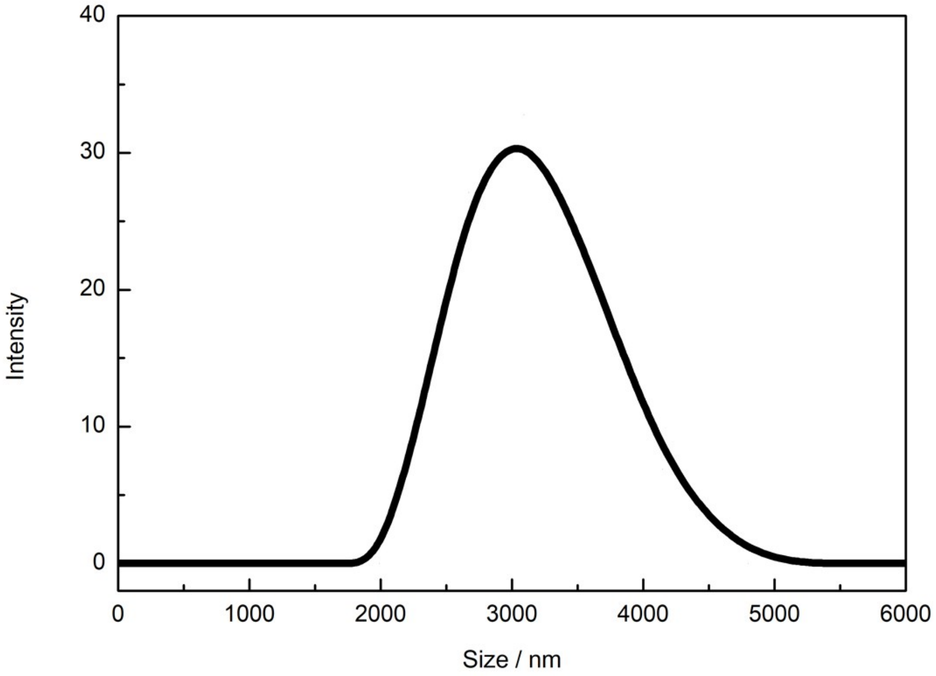

Fig. 40 DLS result of **H⊃G2**.

Reference

S1. Y. Ma, X. Ji, F. Xiang, X. Chi, C. Han, J. He, Z. Abliz, W. Chen and F. Huang, *Chem. Commun.*, 2011, **47**, 12340–12342.

S2. X.-B. Hu, Z. Chen, L. Chen, L. Zhang, J.-L. Hou and Z.-T. Lia, *Chem. Commun.* 2012, **48**, 10999–11001.

S3. Y. Ma, J. Yang, J. Li, X. Chi and M. Xue, *RSC Adv.*, 2013, **3**, 23953–23956.